Journal of Molecular Liquids 387 (2023) 122644

Contents lists available at ScienceDirect

Journal of Molecular Liquids

journal homepage: www.elsevier.com/locate/molliq

Influence of various colloidal surfactants on the stability of MS2 bacteriophage suspension. The charge distribution on the PCV2 virus surface

Natalya Vodolazkaya [a,*], Anna Laguta [a,b], Vladimir Farafonov [a,b], Marina Nikolskaya [a], Zita Balklava [c], Reza Khayat [d], Michael Stich [b,e], Nikolay Mchedlov-Petrossyan [a], Dmitry Nerukh [b]

[a] Physical Chemistry Department, V.N. Karazin Kharkiv National University, Svoboda Sq. 4, Kharkiv 61022, Ukraine
[b] Department of Mathematics, Aston University, Birmingham B4 7ET, UK
[c] College of Health and Life Sciences, Aston University, Birmingham B4 7ET, UK
[d] Department of Chemistry and Biochemistry, City College of New York, New York 10031, United States
[e] Departamento de Matemática Aplicada, Ciencia e Ingeniería de Materiales y Tecnología Electrónica, Universidad Rey Juan Carlos, 28933 Móstoles, Madrid, Spain

ARTICLE INFO

Keywords:
MS2 bacteriophage
PCV2 capsid
Hydrodynamic diameter
Zeta-potential
Surface electrostatic potential
Charge distribution on capsid surface

ABSTRACT

To understand virus stability in aqueous solutions, the colloidal nanostructure and properties of a model virus, the MS2 bacteriophage, have been investigated by studying the effect of the addition of electrolytes and various colloidal surfactants to its water solution at physiological conditions. The charge of the virus particles influences their colloidal properties. It was found that the ζ-potential value is reduced from –35 mV to –10 mV in 0.01 M $CaCl_2$ and 0.1 M NaCl solutions as well as at higher electrolytes concentrations, while the size of the MS2 aggregates was about 600 ÷ 900 nm with individual particles of size around 30 nm also recorded. The 2 : 1 electrolyte causes destabilization of MS2 bacteriophage particles in an aqueous solution at a lower concentration. The addition of cationic, anionic, and non-ionic colloidal surfactants below and above critical micelle concentration to MS2 bacteriophage suspension caused the destabilization of MS2 particles. We also investigated the capsid's surface of another virus, PCV2, using dynamic light scattering and laser Doppler electrophoresis. The hydrodynamic diameter and the ζ-potential of PCV2 empty capsid were found to be equal to 22 ± 1 nm and −41 ± 4 mV (using Ohshima approximations). The electrostatic potential of the surface was measured using acid-base probes and found to be equal to −91 ± 3 and +14 ± 2 mV for positively and negatively charged probes respectively, which indicate the 'mosaic' way of the charge distribution on the surface, similar to MS2's surface studied previously. Our data provide new information about the virus surface, the complex process of virus aggregation-disaggregation and virus capsid disassembly.

1. Introduction

In our previous investigation [1] we have shown that (i) the hydrodynamic diameter and the ζ-potential of MS2 bacteriophage particles at the concentration of 5×10^{11} particles per mL and ionic strength 0.03 M were 30 nm and −34 mV (using Ohshima approximations) respectively, using the dynamic light scattering method and electrophoresis; (ii) the electrostatic potential, Ψ, of MS2 capsid was −50 mV or +10 mV, depending on the molecular probes, which show the 'mosaic' way of the charge distribution on the MS2 surface and (iii) the surface of the MS2 virus was hydrophilic in solution. The effect of adding salts (NaCl and $CaCl_2$) on the aggregation of MS2 suspension was also studied.

The aim of the present investigation is (i) to analyze the colloidal stability of MS2 bacteriophage in aqueous solutions by the combination of electrophoretic and dynamic light scattering in the presence of various colloidal surfactants and compared to the influence of salts (NaCl and $CaCl_2$), which can help in practical formulations for virus inactivation, (ii) to investigate the capsid surface of another virus, porcine circovirus type 2 (PCV2), and to obtain the information about the virus size and distribution of surface charge estimating the local

* Corresponding author.
E-mail address: vodolazkaya@karazin.ua (N. Vodolazkaya).

https://doi.org/10.1016/j.molliq.2023.122644
Received 27 February 2023; Received in revised form 16 July 2023; Accepted 19 July 2023
Available online 22 July 2023

electrostatic potential of the surface Ψ, (iii) to compare the surface properties of MS2 phage and PCV2 as VLP to find a similarity of the viruses' behaviour in aqueous solutions and a possible way of their destruction.

1.1. MS2 bacteriophage and PCV2 virus

MS2 is an icosahedral bacteriophage infecting Gram-negative bacteria (*Escherichia coli*) [2–5] and consisting of a protein outer layer (capsid) and encapsulated internal 3569 nucleotides long single-stranded RNA genome partly bound to the capsid [6–8]. The genomic RNA contains one maturation protein and 89 dimers of the coat protein, which self-organize in a shell structure. The diameter of the capsid is about 28 nm and its thickness is about 2.5 nm. The diameter of the pores in the capsid wall is around 1.1 nm [9]. More detailed information about MS2 bacteriophage can be found in our recent paper [1]. In particular, the isoelectric point of MS2 phage is about 2.2–3.9 and at pH $\leq$ 4 MS2 particles are not stable for aggregation; MS2 bacteriophage is commonly used as surrogates to evaluate pathogenic virus behaviour in natural aquatic media and as a quantitative marker for the effectiveness of antiviral and antiseptic agents. It is mentioned that the electrophoretic mobility of MS2 is systematically negative and the magnitude of the electrophoretic mobility decreases with increasing salt concentration as a result of the screening of the virus charge by the ions present in the electrolytic medium.

Porcine circoviruses (PCV) are a group of four single-stranded DNA viruses that are non-enveloped with a nonsegmental single-stranded DNA genome [10]. PCVs are members of the genus Circovirus which can infect pigs. The viral capsid of PCV type 2 (PCV2) is icosahedral and it is approximately 20 nm in diameter [11].

In [12] the authors reported the 2.3-Å crystal structure of the PCV2 consensus sequence (PCV2CS) virus-like particle. The crystal structure provides the first atomic description for the *Circovirus* family. Molecular Dynamics (MD) and hybrid Molecular Dynamics/hydrodynamics modelling [11] show that the capsid is stable in water solution at room temperature and ion composition similar to physiological conditions. The results of MD simulations of PCV2 viral capsid were presented in [13] investigating the ion distribution on the inner surface of the capsid's wall. Local regions highly occupied by chloride ions were found despite a largely uniform electrostatic potential everywhere on the surface [13]. The regions are located close to the cracks between the capsid proteins that are formed when the capsid is destabilized and thus could initiate the collapse of the capsid [13]. This happens if these regions are depleted of the negatively charged groups (chloride ions or phosphate groups of the genome). The results of MD simulations demonstrated the connection between the number of ions inside a PCV2 empty capsid and its stability [14], an analysis that cannot be done experimentally due to insufficient resolution. It was also found that the chloride ions play a key role in the stability of the capsid [14].

1.2. Virus stability in aqueous solutions

From the colloid chemistry point of view viruses in solution can be described as a self-assembled lyophilic colloidal system. The particles are formed spontaneously through a self-assembling process. The main characteristics of lyophilic colloids are (i) that dispersed particles have a strong affinity to the dispersion medium resulting from the formation of hydrogen bonds; (ii) they are reversible; (iii) their aggregative and kinetic stability can be estimated.

The interfacial interactions of nanoparticles and the aggregation of aqueous dispersions are described by the classical Derjaguin–Landau–Verwey–Overbeek (DLVO) theory that quantifies the balance between the van der Waals interactions and the electrostatic interactions. As a first approximation, the interfacial interactions of spherical virus nanoparticles such as MS2 have been modelled within the DLVO paradigm when investigating the deposition of viruses onto mineral surfaces. DLVO-like interactions have also been successful in describing the bacteriophage PRD1 [15]. However, the complex interactions implicit in these systems often cannot be described using such models where a synergistic combination of steric and electrostatic interactions must be invoked [15]. In a more general context, DLVO theory itself is an approximation not intended for universal application [15].

It should be noted that several environmental factors affect virus – virus interactions and their aggregation state, such as salt concentration, its type (monovalent, divalent), and the presence of natural organic matter [16]. Also, pH- triggered MS2 bacteriophage aggregation was found [16]: the composition of the virus influences its electric charge, resulting in a wide range of isoelectric points. The electrical charge of the particles influences their colloidal properties.

It was noticed [17] that virus aggregation – disaggregation is a complex process and predicting the behaviour of any individual virus is difficult under a given set of environmental conditions without actual experimental data. The authors also mention that these aggregates may behave very differently compared to those formed in suspension by the manipulation of pH and salt concentration in the laboratory [17]. For example, viruses like MS2 adopted similar strategies for stability against aggregation, including the net negative charge in natural water conditions and using polypeptides that form loops extending from the surface of the protein capsid for stabilization. In natural systems, dissolved organic matter can adsorb to and effectively functionalize the nanoparticle's surface, affecting the fate and transport of these nanoparticles [17].

In [18] the authors reported that they manipulated the concentrations of several common media components, including salt, protein, and surfactant, as well as pH, over environmentally and physiologically relevant ranges while quantifying the viability of model viruses in droplets of the media. Also, they noted [18] that the physical behaviour of viruses, such as forming aggregates and partitioning at the air – liquid interface, resulting from changes in droplets' characteristics may also affect inactivation.

It was found [15] that in LiCl, NaCl, and KCl electrolyte solutions, the aggregation of MS2 could not be caused within a reasonable kinetic time frame, and the MS2 solution was stable even at salt concentrations >1.0 M. It has been reported [15] that even at high Ca^{2+} concentrations, diffusion-controlled aggregation was not achieved. However, in our previous investigation [1] and in the discussion of the present study we found some peculiarities of the influence of NaCl and $CaCl_2$ salts on the colloidal stability of MS2.

Cationic, anionic, and non-ionic colloidal surfactants are applied in daily life as liquid soaps, dish detergents, and antimicrobials in many cleaning products. The non-ionic surfactants are used in many processed food and drink products. Therefore, the fundamental understanding of the colloidal interactions between virus particles and colloidal surfactants will help in practical formulations for virus inactivation.

1.3. Acid-base molecular probes used for estimating the electrostatic potential Ψ of the nanoparticles' surface

The investigation of nanoparticles' surface can be carried out using acid-base molecular probes (indicator dyes) of various charge types, sizes, and structures. Their acid-base properties (pK_a) and spectral characteristics are very sensitive to the microenvironment in an aqueous solution containing nanoparticles. The electrostatic potential of the surface Ψ is estimated using the electrostatic theory describing protolytic equilibria in lyophilic colloidal dispersions.

The key characteristic of a pH-dependent indicator dye H_jR^z dissolved in media containing nanoparticles is the so-called 'apparent' dissociation constant, pK_a^a, as defined by equation (1) [1,19,20]:

$$pK_a^a = pH_w + \log \frac{[H_jR^z]}{[H_{j-1}R^{z-1}]} \quad (1)$$

where the ratio of the equilibrium concentrations of H_jR^z and $H_{j-1}R^{z-1}$ is determined UV–Vis spectroscopically; the pH_w values utilized in calculations characterize only the bulk phase and are measured with a glass electrode. Hence, pK_a^a value is an 'instrumental' parameter that can be observed as a constant of the two-phase equilibrium between the nanoparticle surface and the bulk phase. In general, some fraction of indicator species can remain in the bulk phase. To ensure complete binding, ionic indicators with a charge opposite to that of the particle's surface can be used.

According to the electrostatic theory, the apparent value pK_a^a of an indicator under conditions of complete binding depends on the transfer activity coefficients, γ_i, and the electrostatic potential of the surface [1,19,20]:

$$pK_a^a = pK_a^w + \log\left({}^w\gamma^m_{H_{j-1}R^{z-1}} / {}^w\gamma^m_{H_jR^z}\right) - \Psi F/(2.303RT) \quad (2)$$

where pK_a^w – the pK_a value in water; γ_i – the activity coefficients of the species from water to the surface; Ψ – the electrostatic potential of the surface where molecular probes are located; F – the Faraday constant; R – the gas constant; T – the absolute temperature. The agreed notation of the first two terms in equation (2) is pK_a^i, the 'intrinsic' constant. The physical sense of pK_a^i can be expressed as pK_a^a of the molecular probes at $\Psi \to 0$.

Compared to the values in pure water the following pK_a differences are calculated:

$$\Delta pK_a^a = pK_a^a - pK_a^w = \log\left({}^w\gamma^m_{H_{j-1}R^{z-1}} / {}^w\gamma^m_{H_jR^z}\right) - \Psi F/(2.303RT) \quad (3)$$

The so-called 'medium effect' is specified by interfacial solvation and electrostatic effect [1,19,20].

Equation (3) can be converted into the formula for the estimation of the electrostatic surface potential:

$$\Psi = 59 \times \left(pK_a^i - pK_a^a\right), \text{ in mV at } 25^\circ C \quad (4)$$

Thus, it is relevant to investigate (i) the colloidal stability of MS2 bacteriophage in aqueous solutions at additions of various colloidal surfactants and (ii) the PCV2 capsid surface by using dynamic light scattering (DLS) method, laser Doppler electrophoresis, and acid-base probes to estimate the local electrostatic potential of the surface Ψ.

2. Experiment

2.1. Production and purification of MS2 phage and PCV2 capsid

The bacteriophage MS2 (ATCC 15597-B1) and its host *Escherichia coli* (*E. coli*) strain C-3000 (ATCC 15597) were obtained from American Type Culture Collection (ATCC), followed by their propagation, expression, and purification as described below. For the MS2 phage production and purification were used $CaCl_2$ (USP grade), $MgCl_2$ (analytical grade), TRIS (ultrapure), and NaCl (analytical grade) from Melford Laboratories, UK. All chemicals were used without additional purification.

Bacteria *E. coli* were cultured in Lennox L Broth medium (Melford Laboratories) at 37°C and infected with MS2 phage at middle log-phase. The lysate was centrifuged at 10,000 g for 15 min to remove cell debris after complete lysis of the bacteria. MS2 from the supernatant was concentrated using an Amicon Ultra-15 centrifugal filter unit containing Ultracel 100 kDa membrane and then centrifugated again at 100,000g at 4°C for 4 h to pellet the phage particles [21].

The MS2 pellet was resuspended in a buffer solution containing 50 mM TRIS (pH = 7.5), 150 mM NaCl, 5 mM $MgCl_2$, and 5 mM $CaCl_2$. The initial ionic strength of obtained MS2 solution was 0.18 M.

The working suspensions of MS2 phages were kept at 4 °C before use.

PCV2 capsid protein (CP) was purified as previously described [12]. Briefly, a codon-optimized gene for the capsid protein (GenBank: JF504708) was synthesized (DNA 2.0, Menlo Park, Ca). The 41 amino acids at the *N*-terminus were removed and the remaining portion was cloned into a Top10/pET100 vector. The resulting gene product possesses a hexahistidine and a thrombin cleavage site at the *N*-terminus and amino acids 41–231 of PCV2b. Plasmid was transformed into Escherichia coli BL21(DE3) Star strain (Invitrogen). Cells were grown at 37°C till mid-log phase, the temperature was reduced to 20°C, and expression was induced by the addition of 300 μM isopropyl-β-d-thiogalactoside for less than 16 h. Cells were suspended in 20 mM *N*-cyclohexyl-3-aminopropanesulfonic acid [CAPS] (pH = 10.5), 0.5 M NaCl, 50 mM imidazole (pH = 10.5), 0.2 mM phenylmethylsulfonyl fluoride [PMSF], 4 mM β-mercaptoethanol [β-Me], and 20 units of benzonase [EMD4Biosciences]), and lysed using sonicating. The lysate was centrifuged for 30 min at 4°C, 16,000*g*. Nucleic acid was precipitated using a 2 % streptomycin sulfate cut. CP was purified using nickel-nitrilotriacetic acid (Ni-NTA) resin (Qiagen) according to the manufacturer's protocol, dialyzed overnight in lysis buffer containing 20 mM CAPS (pH = 11.1) and supplemented with 200 mM L-Arg (pH = 11.1). CP was concentrated to 50 mg/mL, flash frozen in N_2(l), and stored at −80°C. Protein concentration was determined using the method of Gill and von Hippel [22].

Virus-like particles (VLP) were assembled as previously described [23]. Briefly, CP was diluted to 3 mg/mL in the storage buffer. Capsids were assembled using a 1:1 ratio of CP to 12 % polyethylene glycol (PEG) 3350, 5 % isopropanol, and 0.6 M ammonia citrate (pH = 5). VLPs assemble and form crystals in this condition after two days of incubation at 4°C. Centrifugation at 14,000g for 10 min at 4°C pelleted the crystals. Crystals were suspended and dissolved in 0.3 M 4-(2-hydroxyethyl)-1-piperazinepropane sulfonic acid (HEPPS), pH = 9.0, 0.6 M NaCl, and 5 mM β-mercaptoethanol (β-Me) and processed through a HiPrep 16/60 Sephacryl S-500 HR column (GE Healthcare Life Sciences) equilibrated with 20 mM HEPPS pH 9.0, 0.6 M NaCl, and 5 mM β-Me. The elution, a single peak, was concentrated to 0.2 mg/mL using a 100-kDa MWCO ultrafiltration device (Pall Corporation). VLP condition was assessed using negative stained electron microscopy. Briefly, 3 μL of the sample was applied to recently glow-discharged carbon-coated 400-mesh copper grids (catalog number 01814-F; TedPella), stained with 2 % uranyl formate, and imaged using a JEOL JEM-1230 microscope operating at 120 kV equipped with a Gatan US-4000 charge-coupled device.

2.2. Infectivity analysis

Infectious MS2 phages were counted by plaque analysis method using the double-agar-layer technique. Ten-fold serial dilutions of the MS2 stock solutions were made to the appropriate dilution in the LB medium. Concentrations of infective MS2 phage were measured as the number of plaque-forming units per mL (pfu/mL). The final concentrations of purified phages were 10^{14} pfu/mL and 10^{15} pfu/mL.

The infectivity analysis was used for the estimation of pfu with an error of 10^2. With each step of purification and concentration, the pfu increased confirming the presence of concentrated and viable phage.

The MS2 amount (10^{14} pfu/mL) was also quantified using the Lowry method and expressed in mg protein per mL [21,24]. The total protein concentration according to this method was 16.5 ± 0.6 mg/mL. The estimated total molecular weight of a single MS2 was 3.6×10^6 g/mol [25].

2.3. Materials, procedure and methods of preparing colloidal samples

The samples of the indicator dyes were of high-purity grade. The colloidal surfactants were cetyltrimethylammonium bromide (CTAB) and Triton X-100 (TX-100), 99.0 % from Sigma; sodium *n*-dodecylsulfate (SDS) 99.0 % from Vekton. The surfactants were used without further purification. The chemical formulas of cationic, anionic and non-ionic surfactants and their critical micelle concentration (*cmc*) at 25 °C are given below respectively:

$C_{16}H_{33}\overset{+}{N}(CH_3)_3Br^-$, $cmc = 8 \times 10^{-4}$ M; n-$C_{12}H_{25}OSO_3^-Na^+$, $cmc = 9$

$\times 10^{-3}$ M.

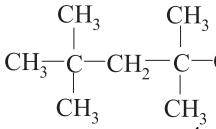

where x = 9–10; $cmc = 2.2 \times 10^{-4}$ M.

The standard NaOH aqueous solution was kept protected from the atmosphere. Aqueous hydrochloric, phosphoric and acetic acids; sodium chloride and borax were of analytical grade.

Suitable pH values of the working solutions used for the pK_a^a measurements were provided by acetate, phosphate, and borate buffer solutions. All solutions were prepared with double distilled water (18.2 MOhm × cm at 25°C). Stock solutions of the dyes were prepared using water as solvent.

The working solutions for pK_a^a measurements were prepared by mixing in 10 mL volumetric flask appropriate aliquots of indicator dyes, buffer components, sodium chloride to keep constant ionic strength (4.5×10^{-3} M) and 0.05 mL PCV2 suspension (200 times dilution, protein concentration is 0.001 mg/mL).

The Vis-absorption spectra were measured using a spectrophotometer Hitachi U-2000 against solvent blanks. The pH measurements were performed using an ESL-63-07 glass electrode and an Ag/AgCl reference electrode in a cell with liquid junction (1 M KCl) at 25.0 ± 0.1°C, using a potentiometer P 37–1; a pH-meter pH-121 served as a nil-instrument. The standard deviation of pH values is ±(0.01–0.02). The cell calibration was performed using standard buffers (pH = 1.68, 4.01, 6.86, and 9.18) at 25°C.

2.4. Size and electrophoretic mobility (ζ-potential) measurements

The measurements of MS2 hydrodynamic size and ζ-potential were performed at 25 °C by dynamic light scattering (DLS) method and laser Doppler electrophoresis using Zetasizer Nano ZS analyzer, He–Ne red laser, wavelength 633 nm (Malvern Instruments, UK), equipped with Dispersion technology and light scattering software.

In the instrument various algorithms are used to analyze the correlation function G(τ) of the scattered intensity, the cumulants and the distribution analyses. The cumulants analysis is a single exponential fit to the autocorrelation function, giving the value of the polydispersity index (PdI) as a criterion for the width of the distribution, but not the size distribution or the Z average. The calculations for these parameters are defined in the ISO standard documents 13,321 and 22,412. The distribution analysis uses a multiple exponential to fit the correlation function to obtain the distribution of particle sizes but it does not provide the PdI value. In this method, PdI is not required because the obtained distributions, based on the number of peaks, can be used to estimate the polydispersity of the system. The first-order result from a DLS experiment is the intensity distribution of particle sizes. The intensity distribution is weighted according to the scattering intensity of each particle fraction. The volume and number distributions demonstrate the total volume and the number of particles in various-size bins, respectively.

Regarding the scattering angle, Malvern Company took into account all the points that could be associated with it. The Zetasizer Nano ZS measures the intensity of scattered light at an angle of 173° due to conventional factors row.

In these experiments, the viral concentration ranged from $\sim 5 \times 10^{11}$ to 5×10^{12} pfu/mL to obtain enough signal from the Zetasizer instrument. Usually, the solutions were not filtered before use. However, special experiments of size and ζ-potential measurements were conducted where the solutions were filtered through a 0.22 μm nylon membrane syringe filter to be sure that the not filtered samples do not influence the results. For size and electrophoretic mobility, the measurements were obtained using three independent experiments with triplicate or more measures in each to ensure the reproducibility of the measurements.

3. Results and discussion

3.1. The measurements of size and zeta-potential of MS2 bacteriophage by DLS method and laser Doppler electrophoresis showing aggregative stability of MS2 bacteriophage suspension

3.1.1. The effect of adding inorganic electrolytes

The main characteristics of colloidal particles in solutions are their size and surface potential, in particular, the ζ-potential, as they allow to predict the aggregative and kinetic stability of the colloids, the coagulation process, the binding of substrate by surface, etc. At present such information for different kinds of colloidal particles is available for many systems, however, the knowledge on the size and ζ-potential of biological nanoparticles, such as viruses, is much less complete [15–18]. The work [26] demonstrates that stability and electrohydrodynamics of MS2 and VLPs differ according to different purifications and the last ones are a so-far overlooked key matter of concern when evaluating physicochemical properties of virus surfaces for predicting their behaviour in aquatic media. Such important information can be used to determine whether the virus particles will be aggregated, dispersed or disassembled at each pH, inorganic electrolytes or surfactant concentrations, etc. In the following, we present the investigation of these parameters using the DLS method and laser Doppler electrophoresis. The ζ-potential of the particle can be obtained using an equation, which was proposed initially in a complete form by Henry and later expressed by Ohshima. A detailed description of the approximations for ζ-potential is given in our paper [1].

The influence of inorganic 1 : 1 and 2 : 1 electrolytes (NaCl and $CaCl_2$) on the stability of MS2 bacteriophage suspension was examined in our previous investigations [1]. We have shown that varying the ionic strength of MS2 solution (5×10^{11} particles per mL) by NaCl in wide range ($9 \times 10^{-4} \div 0.8$ M) did not change the particle's hydrodynamic size significantly. The hydrodynamic diameter of individual particles for all NaCl concentrations was 30 nm by intensity; 25 nm by volume; 20 nm by number. The size of the aggregates was ~600 nm by intensity; ~700 nm by volume. After two weeks at 4 °C the size of the aggregates in the same solutions increased to ~900 nm, but individual particles were also recorded with a size of ~30 nm. For the ζ-potential measurements at varying ionic strength by NaCl, we obtained the following results [1]. In the range of NaCl concentration from 0.06 to 0.8 M only one peak was recorded on the distribution curve at ~−9 mV. We relate this peak to MS2 aggregates of 600 nm size. However, the peak at ~−35 mV observed in the range of 0–0.03 M NaCl concentrations corresponded to individual particles disappearing. Thus, the aggregative stability of the system was reduced at increasing NaCl concentration due to the neutralization of the MS2 bacteriophage surface.

We also varied the ionic strength of the MS2 solution (5×10^{12} particles per mL) by $CaCl_2$ from 9×10^{-4} M to 0.01 M [1]. The size of the individual particles and the existing aggregates were 33 and 450 nm by intensity respectively. The change of salt concentration in a wide range did not influence significantly the hydrodynamic size of the individual particles but increased the fraction of MS2 aggregates. The influence of $CaCl_2$ salt on the ζ-potential value was expected because of the larger cation charge compared to the one–one electrolyte NaCl. For example, the ζ-potential was about –10 mV both at 0.01 M $CaCl_2$ and at 0.1 M NaCl concentrations which is explained by the enhancement of the screening of the surface charge by Ca^{2+}.

It should be noted here that the virus particles have protrusions and are porous, so it is not expected that they precisely follow DLVO theory [15].

3.1.2. The effect of additions of various colloidal surfactants

In this investigation, we have studied the influence of adding various widespread colloidal surfactants by the measurements of size and

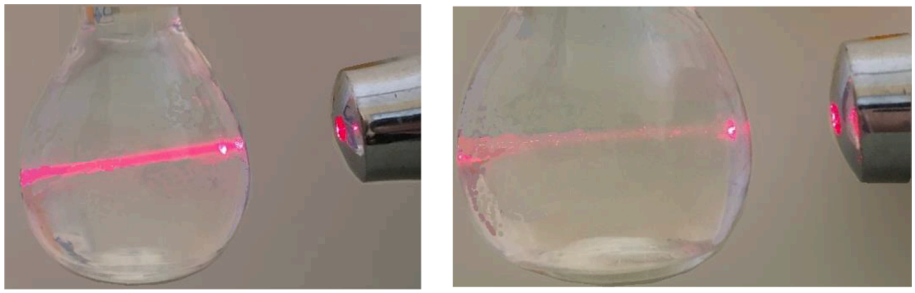

a ***b***

Fig. 1. MS2 solution at concentration 5×10^{11} virus particles per mL with the addition of surfactants. (***a***) 2×10^{-4} M (below *cmc*) cationic surfactant cetyltrimethylammonium bromide. (***b***) 2×10^{-3} M (below *cmc*) anionic surfactant sodium *n*-dodecylsulfate.

ζ-potential of MS2 bacteriophage by DLS method and laser Doppler electrophoresis. The chemical formulas of cationic, anionic, and non-ionic surfactants and their *cmc* are presented in section 2.3. These surfactants are commonly used in daily life. For example, SDS as the anionic surfactant is used in liquid soaps, dish detergents, and other household products; CTAB (cationic surfactant) as an antimicrobial in many cleaning products; the non-ionic surfactants are extensively used in many processed food and drink products as well as in detergents. Consequently, the fundamental understanding and control of colloidal interactions between virus particles and surfactants will aid in practical formulations for virus inactivation and their removal from surfaces.

The antiviral effect depends both on the virus and the structure of the antimicrobial compounds as it was shown in the work [27]. For example, the antiviral activity of CTAB was impaired in acid pH and with an increase of the ionic strength because of viral aggregation, in particular, the MS2 aggregation. This could explain why MS2 was not affected by environmental factors.

The impact of SDS above the CMC on the electrophoretic mobility of MS2 phage was examined [28] and it was shown that the absolute electrophoretic mobility of the MS2 particles remained unchanged.

It is well known that colloidal surfactants can stabilize nanoparticles, for example by forming mono- or bilayers on the surface [29], or, on the contrary, colloidal surfactants can destabilize the solution of nanoparticles interacting with its surface [20]. Such processes depend on the charge of nanoparticles' surface, their nature and type, and the concentration of surfactants (below or above *cmc*).

It was shown [30] that owing to the net negative surface charge of the Norovirus virus-like particles (VLPs, ***i.e.***, virus capsids) at neutral pH, low concentrations of cationic surfactant tend to aggregate the VLPs, whereas low concentrations of anionic surfactant tend to disperse the particles. Increasing the concentration of these surfactants beyond their critical micelle concentration leads to virus capsid disassembly and breakdown of aggregates [30]. Non-ionic surfactants, however, had little effect on virus interactions and likely stabilize them additionally in suspension. It is very important to note that the surfactants are efficient in disrupting the virus structure only above their *cmc*, because the micelles can solubilize the capsid protein dimers and therefore disassemble the capsid structure as explained in [30]. However, the authors note that the reported data [30] are obtained with reconstituted virus capsids, which are likely to be less stable than the native RNA-containing virus assemblies. Therefore, the charge and aggregation state of real Noroviruses are likely to be similar to the reported ones, the natural virus particles may be more stable against surfactant-driven disassembly. We remark that the MS2 phage as studied in the present work contains the RNA genome inside the capsid.

In [31] the authors posed a question: are proteins denatured by monomeric surfactant molecules, micelles, or both? They have highlighted the role of micelles, rather than monomers in promoting both protein denaturation and the formation of higher-order structures. Also,

Table 1
The hydrodynamic diameter of MS2 particles at 5×10^{12} particles per mL (200-fold dilution of the initial suspension 10^{15} pfu concentration) at the addition of cationic surfactant CTAB to suspensions and polydispersity index, PdI (average PdI value lies in the range 0.08 ÷ 0.7) at 25 °C.

c(CTAB)/M	Diameter/nm				PdI
	by intensity		by volume	by number	
	I Peak	II Peak			
0	34 ± 1	1000 ± 2	27 ± 1	22 ± 1	0.34 ± 0.01
1×10^{-5}	34 ± 1	740 ± 7	27 ± 1	22 ± 1	0.36 ± 0.03
1×10^{-4} *	34 ± 1	600 ± 1	27 ± 1	23 ± 1	0.40 ± 0.04
1×10^{-3} *	1000 ± 1	160 ± 3	1200 ± 3	70 ± 3	0.53 ± 0.02
1×10^{-2} *	710 ± 9	–	1100 ± 7	180 ± 6	0.37 ± 0.04

* The opalescence and turbidity of the solution were observed.

it was reported [32] that the cationic surfactant (didodecyldimethylammonium bromide) above *cmc* (0.016 mM) can deactivate SARS-CoV-2 in as little as 5 s.

As we have shown before [1] using molecular probes the local electrostatic potentials of the MS2 capsid are −50 mV and +10 mV, which show the 'mosaic' way of the charge distribution on the surface. Thus, the cationic surfactant cetyltrimethylammonium bromide (2×10^{-4} M, below *cmc*) and anionic surfactant sodium *n*-dodecylsulfate (2×10^{-3} M below *cmc*) were added to MS2 solution at the concentration 5×10^{11} virus particles per mL. Qualitative observations of these systems showed the following (Fig. 1). The opalescence and turbidity of the solution were observed in the case of CTAB addition as well as Tyndall effect was demonstrated. During two days the turbidity was preserved, but no visible sedimentation. At SDS addition to the MS2 solution the opalescence and turbidity of the solution were not observed, no Tyndall effect and during two days the turbidity did not appear. Thus, the local positive electrostatic potential on the MS2 surface is not significant enough for negatively charged ions of colloidal surfactant to influence dispersion stability.

We further continued the quantitative measurements of these systems by the DLS method and laser Doppler electrophoresis. The data on hydrodynamic diameter and ζ-potential distribution of MS2 solution at the concentration 5×10^{11} virus particles per mL are presented in Tables 1-4 and in the Supplementary Materials as Figures S1-S4.

These data confirm visual observations (Fig. 1). No significant changes in size and ζ-potential at SDS addition to MS2 solution (Tables 3, 4 and Supplementary Materials, Fig. S2, S4) compared to the data without any additions [1]. In the case of 2×10^{-4} M CTAB addition, in the ζ-potential distribution the peak near − 10 mV appeared related to the aggregation of virus particles because of the neutralization of negatively charged MS2 surface and its hydrophobization compared with inorganic electrolytes (Supplementary Materials, Fig. S3).

For a more detailed study of the influence of colloidal surfactant on

Table 2
Electrophoretic mobility (±0.1 μmcm/Vs) and ζ-Potential values (±3 mV) of MS2 particles in aqueous solution at 5×10^{12} particles per mL (200-fold dilution of the initial concentration 10^{15} pfu at $I = 9 \times 10^{-4}$ M*) at the addition of cationic surfactant CTAB to suspensions, 25 °C.

c(CTAB)/M	Electrophoretic mobility / μmcm/Vs		ζ /mV by Smoluchowski ($f = 1.5$)		ζ / mV by Hückel ($f = 1$)		ζ / mV by Ohshima (variable f)	
	I Peak	II Peak	I Peak	II Peak	I Peak	II Peak	I Peak	II Peak
0	–1.9		–24		–36		–34	
1×10^{-5}	–2.0	–0.2	–25	–3	–38	–4	–35	–4
1×10^{-4}	–2.0	–0.5	–25	–7	–38	–10	–35	–10
1×10^{-3}	+1.8		+23		+34		+32	
1×10^{-2}	+2.8		+35		+53		+46	

* Ionic strength of virus solution after dilution. At additions of surfactant ionic strength is increased by corresponding surfactant concentration (below *cmc*) and by *cmc* value (after micelles forming).

Table 3
The hydrodynamic diameter of MS2 particles at 5×10^{12} particles per mL (200-fold dilution of the initial suspension 10^{15} pfu concentration) at the addition of anionic surfactant SDS to suspensions and polydispersity index, PdI (average PDI value lies in the range 0.08 ÷ 0.7) at 25 °C.

c(SDS)/M	Diameter/nm				PdI
	by intensity		by volume	by number	
	I Peak	II Peak			
0	35 ± 1	1000 ± 2	27 ± 1	22 ± 1	0.34 ± 0.01
1×10^{-5}	33 ± 1	620 ± 7	27 ± 1	23 ± 1	0.43 ± 0.02
1×10^{-4}	33 ± 1	780 ± 7	27 ± 1	23 ± 1	0.43 ± 0.01
1×10^{-3}	33 ± 1	700 ± 9	27 ± 1	23 ± 1	0.43 ± 0.03
1×10^{-2}	36 ± 1	2900 ± 3	30 ± 1	26 ± 1	0.60 ± 0.02

Table 4
Electrophoretic mobility (±0.1 μmcm/Vs) and ζ-Potential values (±3 mV) of MS2 particles in aqueous solution at 5×10^{12} particles per mL (200-fold dilution of the initial concentration 10^{15} pfu at $I = 9 \times 10^{-4}$ M*) at the addition of anionic surfactant SDS to suspensions, 25 °C.

c (SDS)/ M	Electrophoretic mobility / μmcm/Vs		ζ / mV by Smoluchowski ($f = 1.5$)		ζ / mV by Hückel ($f = 1$)		ζ / mV by Ohshima (variable f)	
	I Peak	II Peak	I Peak	II Peak	I Peak	II Peak	I Peak	II Peak
0	–1.9	–	–24	–	–36	–	–34	–
1×10^{-5}	–1.7	–	–22	–	–33	–	–30	–
1×10^{-4}	–2.2	–0.9	–28	–11	–42	–17	–39	–16
1×10^{-3}	–2.0	–0.4	–26	–5	–39	–	–36	–7
1×10^{-2}	–2.2	–0.2	–28	–1	–49	–	–37	–1

* Ionic strength of virus solution after dilution. At additions of surfactant ionic strength is increased by corresponding surfactant concentration (below *cmc*) and by *cmc* value (after micelles forming).

MS2 solution stability, we have experimented with varying the concentration of the cationic and anionic surfactant (below and above *cmc*) by DLS method and laser Doppler electrophoresis.

3.1.2.1. The effect of adding cationic surfactants. The data on hydrodynamic diameter and ζ-potential with varying CTAB concentration in the range $1 \times 10^{-5} \div 1 \times 10^{-2}$ M are collected in Tables 1, 2 and in Figures S5, S6 of the Supplementary Materials. When *cmc* value was achieved in the MS2 solution, clear aggregation is observed (Tables 1, 2). The size of particles was dramatically increased and ζ-potential potential changed sign and became positive. For example, we observed earlier the recharge of the surface in the system consisting of negatively charged silica nanoparticles after covering by a bilayer of cationic surfactant [29], but in this case, the system was stable. In the present investigation, the bilayer of cationic surfactants on the capsid was not formed because at CTAB concentration below *cmc* the ζ-potential potential stays negative (Table 2) although the evaluated quantity of CTAB is about 1×10^{-4} M to form bilayer on the virus surface at 5×10^{12} MS2 particles per mL. Also, at such CTAB concentration, the colloidal stability of MS2 solution was lost to some extent because the opalescence and turbidity of the solution were observed (Table 1). The cationic surfactant at concentrations below *cmc* may reduce the magnitude of the apparent capsid surface charge enough to induce the beginning of MS2 particle aggregation [30] (Table 2, ζ = –35 and –10 mV). Above *cmc* the micelles can solubilize capsid protein dimers and therefore disassemble the capsid structure (Table 2) [30].

Table 5
The hydrodynamic diameter of MS2 particles at 5×10^{12} particles per mL (200-fold dilution of the initial suspension 10^{15} pfu concentration) at the addition of non-ionic surfactant Triton X-100 to suspensions and polydispersity index, PdI (average PDI value lies in the range 0.08 ÷ 0.7) at 25 °C.

c(TX-100)/M	Diameter/nm				PdI
	by intensity		by volume	by number	
	I Peak	II Peak			
0	34 ± 1	1000 ± 2	27 ± 1	22 ± 1	0.34 ± 0.01
1×10^{-2}	30 ± 1	940 ± 9	5.9 ± 0.5	5.9 ± 0.5	0.54 ± 0.03

3.1.2.2. The effect of adding anionic surfactants. The data on hydrodynamic diameter and ζ-potential with varying SDS concentration in the range $1 \times 10^{-5} \div 1 \times 10^{-2}$ M are collected in Tables 3, 4 and in Figures S7, S8 of the Supplementary Materials. As we can see no significant change in the size and ζ-potential at SDS addition (below and above *cmc*) to the MS2 solution compared to the data without any additions was observed [1]. The SDS had the same sign of charge as the MS2 capsid. Hereby, no influence of SDS monomers or micelles on the stability of the MS2 virus was detected. The local positive electrostatic potential on the MS2 surface was low by absolute value (+10 mV) [1] such that the electrostatic interactions between these positively charged parts and negatively charged SDS monomers could cause an insignificant increase in the magnitude of apparent surface charge. The SDS micelles also did not interact with the MS2 virus and even they have repulsion from negatively charged MS2 surfaces (Tables 3, 4).

3.1.2.3. The effect of adding non-ionic surfactants. The data on hydrodynamic diameter and ζ-potential at the addition of non-ionic surfactant Triton X-100 above *cmc* are presented in Tables 5, 6 and in Figs. 2, 3. Interesting to note that only in this case particles with a size of about 6 nm by volume and by number which can be referred to the size of non-ionic micelles (Fig. 2) were detected. Micelles would be the only particles represented in a volume distribution, where $V \sim r^3$. At the same time from DLS data by intensity it is observed the following picture for MS2

Table 6
Electrophoretic mobility (±0.1 μmcm/Vs) and ζ-Potential values (±3 mV) of MS2 particles in aqueous solution at 5×10^{12} particles per mL (200-fold dilution of the initial concentration 10^{15} pfu at $I = 9 \times 10^{-4}$ M) at the addition of anionic surfactant Triton X-100 to suspensions, 25 °C.

c(TX-100)/M	Electrophoretic mobility / μmcm/Vs		ζ / mV by Smoluchowski ($f = 1.5$)		ζ / mV by Hückel ($f = 1$)		ζ / mV by Ohshima (variable f)	
	I Peak	II Peak	I Peak	II Peak	I Peak	II Peak	I Peak	II Peak
0	–1.9		–24		–36		–34	
1×10^{-2}	–0.6	–1	–7	–24	–11	–35	–10	–33

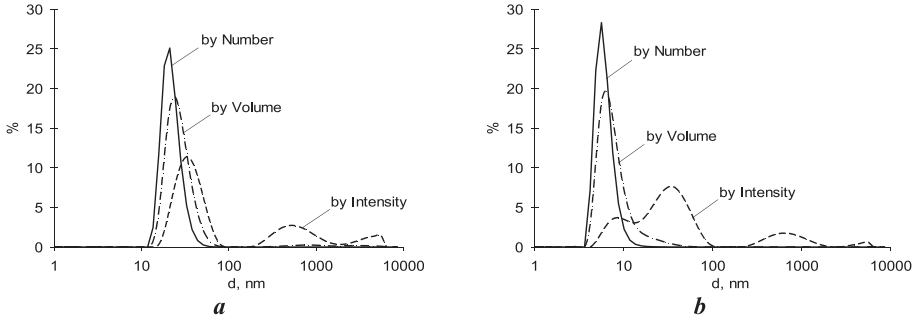

Fig. 2. Size distribution by number, volume, and intensity of MS2 solution at the concentration of 5×10^{12} virus particles per mL (200-fold dilution of the initial suspension 10^{15} pfu concentration) at varying the non-ionic surfactant Triton X-100 concentrations: (***a***) 0; (***b***) 1×10^{-2} M.

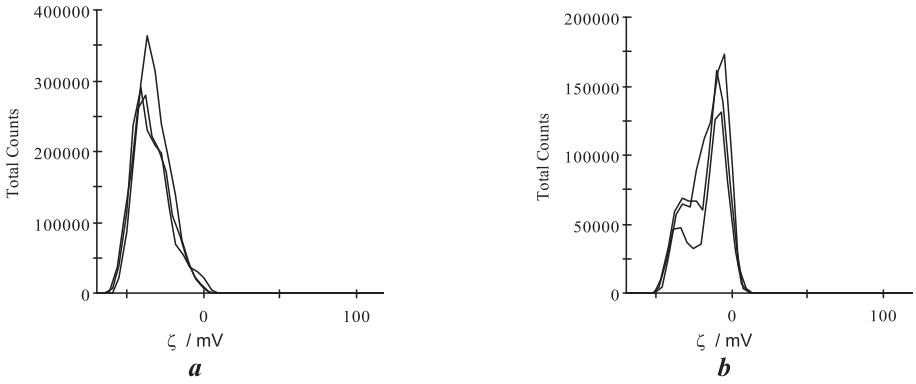

Fig 3. ζ-potential distribution of MS2 aqueous solution at the concentration of 5×10^{12} virus particles per mL (200-fold dilution of the initial suspension 10^{15} pfu concentration) using Ohshima approximations at the addition of non-ionic surfactant Triton X-100 to suspensions: (***a***) 0; (***b***) 1×10^{-2} M. Ionic strength is 9×10^{-4} M.

solution: the virus particles as monomers (~30 nm) and aggregates (~900 nm). However, in Fig. 2 we can see the redistribution of intensity peaks and the aggregates are predominant compared to the MS2 solution without non-ionic additions.

The results of the measurements of the ζ-potential in the MS2 solution with non-ionic micelles contained two peaks compared to the system without surfactant. The first peak was about − 10 mV and the second one was about − 30 mV (Table 6, Fig. 3). Here, such reduction of ζ-potential can be caused by increasing the aggregation of MS2 virus under the influence of non-ionic micelles. The second peak can be attributed to the monomers of MS2 bacteriophage. However, in the study of surfactant-mediated Norovirus interactions [30] it was found that non-ionic surfactants below and above *cmc* had little effect on virus interactions and likely stabilized them in suspension.

3.2. The measurements of size and ζ-potential of PCV2 capsid by DLS method and laser Doppler electrophoresis

The hydrodynamic diameter and the ζ-potential of PCV2 capsid particles were measured at their concentration of 0.002 and 0.001 mg/mL protein concentration and ionic strength 9×10^{-3} and 4.5×10^{-3} M at 100- and 200-fold dilutions of the initial suspension respectively. The data are collected in Tables 7 and 8. In Figs. 4 and 5 the size distribution by intensity, volume, number, and ζ-potential distribution of PCV2 aqueous solution using Ohshima approximations are presented. The

Table 7
The hydrodynamic diameter of PCV2 particles at various dilutions of the initial suspension and polydispersity index, PdI (average PdI value lies in the range 0.08 ÷ 0.7) at 25 °C.

Dilution of PCV2 suspension	Diameter / nm					PdI
	by intensity			by volume	by number	
	I Peak	II Peak	III Peak			
1/100	30 ± 1 (80 %)	250 ± 30 (16 %)	5230 ± 300 (4 %)	20 ± 3	16 ± 1	0.33 ± 0.06
1/200	31 ± 1 (78 %)	278 ± 40 (18 %)	4590 ± 300 (4 %)	21 ± 2	14 ± 1	0.39 ± 0.07
1/200 (filtered)	22 ± 1 (100 %)	–	–	21 ± 1	19 ± 2	0.39 ± 0.07

Table 8
Electrophoretic mobility (±0.2 μmcm/Vs) and ζ-potential values (±4 mV) of PCV2 particles at various protein concentrations in aqueous solution at ionic strength 9×10^{-3} and 4.5×10^{-3} M respectively, 25 °C.

Dilution of MS2 suspension / protein concentration	Electrophoretic mobility / μmcm/Vs	ζ / mV by Smoluchowski ($f = 1.5$)	ζ / mV by Hückel ($f = 1$)	ζ / mV by Ohshima (variable f)
1/100 0.002 mg/mL	–2.3	–30	–45	–41
1/200* 0.001 mg/mL	–1.2	–15	–23	–22

* In this case attenuator index was 11. It denotes no attenuation (full laser power), only high-scattering samples are within acceptable limits.

obtained results of the particle size by the DLS method show polydispersity (PdI > 0.3) of the system at 100- and 200-fold dilutions of the initial suspension.

There are at least 3 types of PCV2 particles in solution: monomers, dimers, and aggregates (Table 7). We assumed from the DLS data that monomers (hydrodynamic diameter, d_h, about 17–20 nm) with some number of dimers ($d_h \sim 30$ nm) were predominant. Our assumption about the dimers was based on the result from the literature [16] where it was shown that the virus dimers of MS2 were detected by cryo-TEM image. The dilutions by 100- and 200-fold of the initial PCV2 suspension did not influence the hydrodynamic size of the virus particles. To compare these data with previous MS2 results [1] where 50, 100, 200, and 400-fold dilution of the MS2 initial suspension (protein concentration of MS2 initial suspension was 16.5 mg/mL) did not change the hydrodynamic size of the individual particles and aggregates. The average hydrodynamic diameter was on the first peak 30 nm by intensity; 20 nm by volume; and on the second peak 300 nm by intensity;

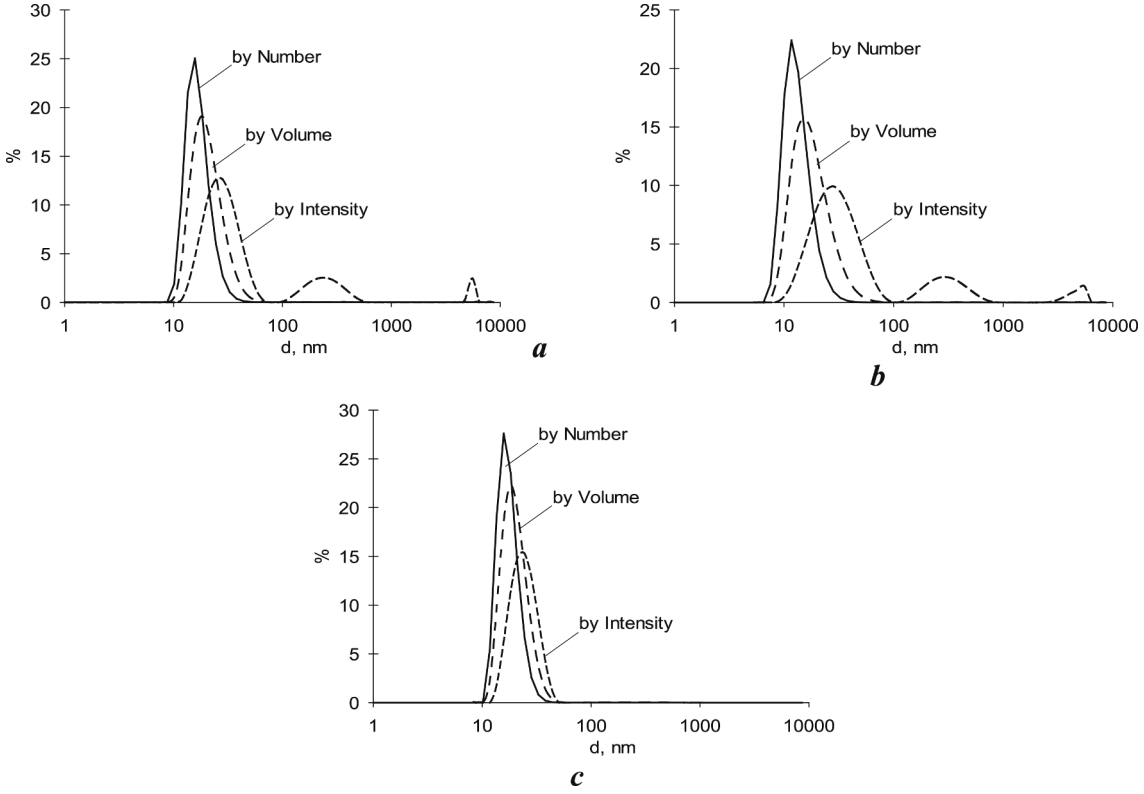

Fig. 4. Size distribution by number, volume, and intensity of PCV2 solution at various dilutions of the initial suspension: (***a***) 1/100; (***b***) 1/200; (***c***) 1/200 (filtered).

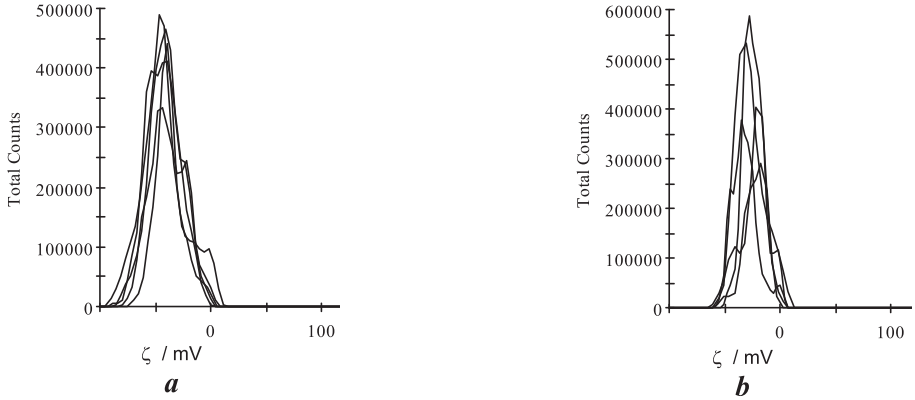

Fig. 5. ζ-potential distribution of PCV2 aqueous solution using Ohshima approximations: (***a***) 1/100; (***b***) 1/200, ionic strength 9×10^{-3} and 4.5×10^{-3} M.

Table 9
The pK_a^a and ΔpK_a^a of indicators in PCV2 solution at concentration 0.001 mg/mL and ionic strength 4.5×10^{-3} M, and the estimated Ψ value of capsid surface at 25 °C.

Type of indicator probe	Indicator / charge type of acid-base couple	pK_a^a	pK_a^{w*} (±0.05)	$\Delta pK_a^a = pK_a^a - pK_a^w$	$pK_a^i - pK_a^{a**}$	Estimated Ψ value from eq. (4) (in mV)
Anionic (~0.9 nm)	γ-Dinitrophenol (0/–)	5.03 ± 0.03	5.22	–0.19	+0.23	+14 ± 2
Cationic (>1.2 nm)	Hexamethoxy red (+/0)	3.65 ± 0.05	3.10	+0.55	–1.55	–91 ± 3

* pK_a^w values of molecular probes were obtained under the same conditions as pK_a^a values in the MS2 solution.
** $pK_a^i = pK_a^a$ value of the same indicator bound by a non-ionic surface. The pK_a^i values are 5.26 and 2.10 for γ-dinitrophenol and hexamethoxy red respectively [20].

500 nm by volume respectively. Thus, the monomers were predominant in the MS2 solution with some number of aggregates.

However, after the filtration of PCV2 suspension at 200-fold dilution and when the major aggregates were separated, we obtained the hydrodynamic diameter of PCV2 particles on average 21 nm by intensity, volume, and number (Table 7). The given size of PCV2 was confirmed by the literature data [11]. Such difference in the size of particles before and after filtration can be explained by the high polydispersity of the system (when three types of aggregates take place) that shifts the results of DLS on the side of increasing size and band broadening.

The obtained ζ-potential values of the PCV2 capsid surface by laser Doppler electrophoresis (Table 8, Fig. 5) are in good agreement with those for MS2 virus particles at neutral pH [1]. The ζ-potential of the MS2 virus particles was measured at their concentration of 5×10^{11} particles per mL and ionic strength of 0.03 M. The values were found to be −29 or −34 mV (by Smoluchowski or Ohshima approximations) respectively [1]. In the case of PCV2 capsid the ζ-potentials were −41 and −22 mV (using Ohshima approximations) 100- and 200-fold dilutions respectively (Table 8). The PCV2 capsid surface was overall negatively charged and the values show that the virus particles were colloidally stable and existed mainly as monomers.

3.2.1. The investigation of the PCV2 virus surface using acid-base indicator dyes: The estimation of the electrostatic potential of the surface Ψ using pK_a values of molecular probes

We have investigated experimentally the PCV2 capsid surface estimating its charge distribution as in the case of MS2 bacteriophage in our previous investigation [1] using acid-base molecular probes (indicator dyes) [19,20].

The main equations describing the behaviour of the molecular probes in solutions containing nanoparticles are given in Introduction (Eq. 1–4). In our case, we assumed that the molecular probes were completely bound due to electrostatic interactions. However, it was difficult to verify this fact for virus suspensions, in contrast to the micellar solutions of surfactants [19,20]. In the latter, it was very easy to vary the micelles concentration and to achieve the constant pK_a^a values of the indicator dyes as evidence of complete binding [19,20].

The electrostatic potential of the surface Ψ can be estimated using the common formula (Eq. (4) in Introduction): $\Psi = 59 \times (pK_a^i - pK_a^a)$, mV at 25 °C [1,19,20]. The pK_a^i value at the ionic surface is often equated to the pK_a^a value of the same indicator bound by non-ionic or zwitterionic surface where $\Psi \to 0$ or to the pK_a^w value in water [19]. We estimated the Ψ values of the virus surface using these three approaches. However, the obtained data show that the best approximation of the pK_a^i value was the pK_a^a value of the same indicator bound by a non-ionic surface. The zwitterionic surface had a chameleon-like nature and the surface could be positively or negatively charged [19]. The approximation of pK_a^i value as pK_a^w value in water was not sufficiently accurate because it did not take into account the transfer activity coefficients (γ_i) of the corresponding species from water to the surface (Eq. (2) in Introduction).

The local Ψ values of the PCV2 particles were examined by molecular probes of various charge types, sizes, and structures to compare with obtained ζ-potential of the virus particle and with another virus, the MS2 bacteriophage. In the latter case, it was found [1], using molecular probes, that the local electrostatic potentials of the MS2 surface were (−50 ± 5) mV and (+10 ± 5) mV, which indicates the 'mosaic' way of the charge distribution on the surface confirming our computer simulation results [9,33].

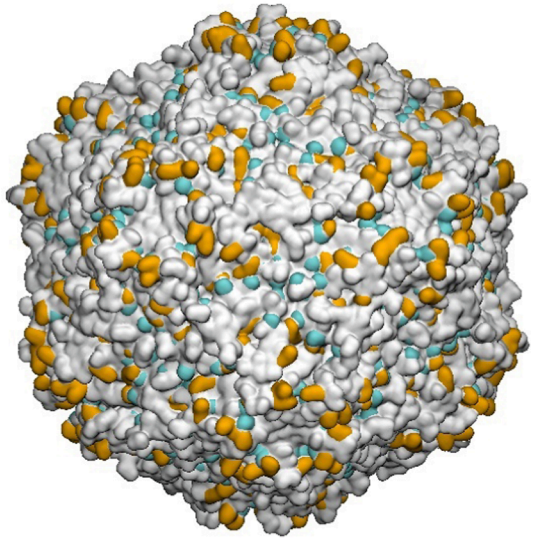

Fig. 6. Mosaic structure of the charge distribution on the PCV2 capsid surface. The anionic glutamate and aspartate residues are colored blue, and the cationic lysine and arginine residues are colored orange.

In general, the surface of the PCV2 capsid is negatively charged according to the data of laser Doppler electrophoresis, and ζ-potential reflects this. However, the molecular probes of various charge types, sizes, and structures in the solutions containing PCV2 particles could be bound by the surface and could give more precise information about the local electrostatic potential. The latter is always higher than the ζ-potential by the absolute value. It also provides more detailed information about the virus's surface.

We examined the pK_a^a values of anionic (~0.9 nm, γ -dinitrophenol) and cationic (>1.2 nm, hexamethoxy red) indicators in a solution containing PCV2 particles with protein concentration 0.001 mg/mL and ionic strength 4.5×10^{-3} M (Table 9). The spectral and acid-base properties of indicators are very sensitive to their microenvironment in aqueous solution [1,19,20].

In both cases, the maxima of the absorption spectra of indicator dyes in PCV2 solutions coincided with those in aqueous solution. This is not typical for molecular probes bound by charged nanoparticles in solutions [19,20]. However, such behavior can be observed on the surface of nanoparticles, if enough water molecules are adsorbed.

Comparing to the pK_a^w values in pure water the following pK_a^a differences were calculated ΔpK_a^a (Eq. (3) (Table 9). They were +0.55 for

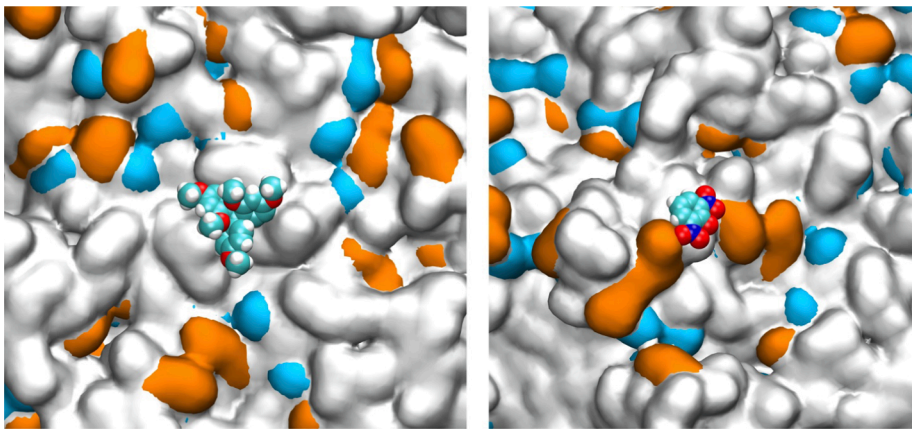

Fig. 7. Schematic assumed localization of the positive, hexamethoxy red (left) and negative, γ-dinitrophenol (right) probes on the surface of the PCV2 capsid. The anionic glutamate and aspartate residues are colored blue, the cationic lysine and arginine residues are colored orange.

the positive probe and −0.19 for the negative probe. This was the so-called medium effect that reflected the influence of solvation and electrostatic influence on the acid-base properties of the molecular probes in solutions containing nanoparticles according to Eq. (3) (see Introduction).

The values of ΔpK_a^a in the virus solutions were positive for positive probes, which is characteristic for negatively charged surfaces and negative for negatively charged probes typical for positively charged surfaces [1,19,20]. The Ψ values on average were −91 mV and +14 mV respectively (Table 9), which indicates the 'mosaic' way of the charge distribution on the surface (Fig. 6) as in the case of MS2 bacteriophage surface [1]. This mosaic character stems from the distribution of the charged amino acid residues across the capsid (Fig. 6).

The sign of Ψ for each probe allows us to suggest its localization on the capsid surface. The inspection of the latter indicates several regions where positively or negatively charged residues are grouped. We assumed them as probable places where the probe molecules could adsorb. They are depicted in Fig. 7 for both probes. We emphasize that this is an illustration based on the results of the experiment. It is not a product of docking or another computational modelling.

We found that the overall ζ-potential of the PCV2 capsid surface was negative, −41 mV (using Ohshima approximations) at 100-fold dilution. However, using acid-base probes we have experimentally detected patches of positive and negative charge on the surface (Fig. 6) and demonstrated their impact on the binding of molecules to the capsid.

It is important that different indicator dyes give positive or negative Ψ values in the same pH range. That is, it is not the effect caused by varying pH, and this is a new result, possibly calling for additional experiments and thinking.

4. Conclusions

We investigated experimentally using physical chemistry approaches the MS2 virus stability in aqueous solutions about the effect of inorganic electrolytes and various colloidal surfactants in water at physiological conditions.

It was found that the ζ-potential value is reduced from –35 mV to –10 mV both at 0.01 M $CaCl_2$ and at 0.1 M NaCl concentrations and higher electrolytes concentrations herewith the size of the MS2 aggregates about 600 ÷ 900 nm, but individual particles were also recorded with the size around 30 nm.

The addition of cationic, anionic, and non-ionic colloidal surfactants below and above critical micelle concentration (*cmc*) to MS2 bacteriophage solutions was investigated. The ζ-potential value was reduced upon the addition of cationic surfactant and even the surface recharge takes place from −25 mV to +35 mV below and above *cmc* respectively as well as MS2 virus aggregation was very clear above *cmc* of CTAB. The addition of anionic surfactant as monomers or in the form of micelles did not show MS2 virus aggregation, dispersion, or disassembly. The presence of non-ionic micelles increased bacteriophage aggregation and reduced the ζ-potential value. Thus, the 2 : 1 electrolyte at low concentrations, and additions of cationic and non-ionic micelles caused the destabilization of MS2 bacteriophage particles in an aqueous solution.

We estimated the particle size and aggregation of porcine circovirus type 2 (PCV2) in solution as well as the ζ-potential and the local electrostatic potential of the surface Ψ and it was compared with those of MS2 bacteriophage.

The hydrodynamic diameter and the ζ-potential of PCV2 empty capsids were 22 nm and −41 mV respectively.

The estimation of the local electrostatic potential of the PCV2 capsid surface using molecular probes (indicator dyes) showed two Ψ values: −91 and +14 mV, which indicated the 'mosaic' way of the charge distribution on the surface similar to the case of MS2 bacteriophage in our previous investigation [1]. The electrostatic potential of virus particles is concluded to be a reliable indicator of the dispersion stability and the key to effective virus aggregation or/and disassembly through the reduction of their Ψ values with coagulants.

Further investigation of such systems using obtained physicochemical data and findings can provide an understanding of how to reduce viral infectivity.

CRediT authorship contribution statement

Natalya Vodolazkaya: Conceptualization, Methodology, Investigation. **Anna Laguta:** Investigation, Data curation. **Vladimir Farafonov:** . **Marina Nikolskaya:** Investigation. **Zita Balklava:** . **Reza Khayat:** . **Michael Stich:** . **Nikolay Mchedlov-Petrossyan:** . **Dmitry Nerukh:** Conceptualization, Methodology.

Declaration of Competing Interest

The authors declare that they have no known competing financial interests or personal relationships that could have appeared to influence the work reported in this paper.

Data availability

Data will be made available on request.

Acknowledgements

N. M.-P. thanks the Ministry of Education and Science of Ukraine for

financial support in the frame of project #0122U001485. A. L. and V. F. thank the Ministry of Education and Science of Ukraine for financial support in the frame of project #0120U101064. V. F. and D. N. acknowledge the use of HPC Midlands supercomputer funded by EPSRC, grant number EP/P020232/1; the access to HPC Call Spring 2021, EPSRC Tier-2 Cirrus Service; the access to Sulis Tier 2 HPC platform hosted by the Scientific Computing Research Technology Platform at the University of Warwick. Sulis is funded by EPSRC Grant EP/T022108/1 and the HPC Midlands + consortium. The collaboration was supported by the program H2020-MSCA-RISE-2018, project AMR-TB, grant ID: 823922. Funds supporting these studies were provided by the NIH National Institute of General Medical Sciences and National Institute of Allergy and Infectious Diseases (5SC1AI114843) and by grant 5G12MD007603-30 from the National Institute on Minority Health and Health Disparities to R. K. Data collection for the VLP assembly was performed at the Simons Electron Microscopy Center and National Resource for Automated Molecular Microscopy, located at the New York Structural Biology Center, supported by grants from the Simons Foundation (349247), NYSTAR, and the NIH National Institute of General Medical Sciences (GM103310).

The authors thank Gorbenko G. P. and her research group (V. N. Karazin Kharkiv National University) for the estimation of MS2 amount (the total protein concentration) using the Lowry method.

Appendix A. Supplementary data

Supplementary data to this article can be found online at https://doi.org/10.1016/j.molliq.2023.122644.

References

[1] N. Vodolazkaya, M. Nikolskaya, A. Laguta, V. Farafonov, Z. Balklava, M. Stich, N. Mchedlov-Petrossyan, D. Nerukh, Estimation of nanoparticle's surface electrostatic potential in solution using acid-base molecular probes III: Experimental hydrophobicity/hydrophilicity and charge distribution of MS2 virus surface, J. Phys. Chem. B. 126 (41) (2022) 8166–8176, https://doi.org/10.1021/acs.jpcb.2c04491.

[2] J.H. Jr, R.L. Strauss, Sinsheimer., Purification and properties of bacteriophage MS2 and of its fibonucleic acid, J. Mol. Biol. 7 (1963) 43–54, https://doi.org/10.1016/S0022-2836(63)80017-0.

[3] B. Hu, P. Khara, P.J. Christie, Structural bases for F Plasmid conjugation and F pilus biogenesis in Escherichia coli, Proc. Natl. Acad. Sci. (PNAS) 116 (2019) 14222–14227, https://doi.org/10.1073/pnas.1904428116.

[4] L. Harb, K. Chamakura, P. Khara, P.J. Christie, R. Young, L. Zeng, ssRNA phage penetration triggers detachment of the F-pilus, Proc. Natl. Acad. Sci. (PNAS) 117 (2020) 25751–25758, https://doi.org/10.1073/pnas.2011901117.

[5] A. Wagner, L.I. Weise, H. Mutschler, InVitro characterisation of the MS2 RNA polymerase complex reveals host factors that modulate emesviral replicase activity, Communications Biology. 5 (2022) 264–275, https://doi.org/10.1038/s42003-022-03178-2.

[6] K. Valegard, L. Liljas, K. Fridborg, T. Unge, The three-dimensional structure of the bacterial virus MS2, Nature. 345 (1990) 36–41, https://doi.org/10.1038/345036a0.

[7] M.R. Machado, S. Pantano, Fighting viruses with computers, right now, Current Opinion in Virology. 48 (2021) 91–99, https://doi.org/10.1016/j.coviro.2021.04.004.

[8] D.T. Le, K.M. Müller, InVitro assembly of virus-like particles and their applications, Life. 11 (2021) 334–353, https://doi.org/10.3390/life11040334.

[9] V. Farafonov, D. Nerukh, MS2 bacteriophage capsid studied using all-atom molecular dynamics, Interface Focus. 9 (2019) 20180081, https://doi.org/10.1098/rsfs.2018.0081.

[10] Y. Zhang, Z. Wang, Y. Zhan, Q. Gong, W. Yu, Z. Deng, A. Wang, Y. Yang, N. Wang, Generation of E. coli-derived virus-like particles of porcine circovirus type 2 and their use in an indirect IgG enzyme-linked immunosorbent assay, Arch Virol. 161 (2016) 1485–1491, https://doi.org/10.1007/s00705-016-2816-9.

[11] E. Tarasova, I. Korotkin, V. Farafonov, S. Karabasov, D. Nerukh, Complete virus capsid at all-atom resolution: simulations using molecular dynamics and hybrid molecular dynamics/hydrodynamics methods reveal semipermeable membrane function, J. Mol. Liq. 245 (2017) 109–114, https://doi.org/10.1016/j.molliq.2017.06.124.

[12] R. Khayat, N. Brunn, J.A. Speir, J.M. Hardham, R.G. Ankenbauer, A. Schneemann, J.E. Johnson, The 2.3-Angstrom Structure of Porcine Circovirus 2, J Virol 85 (15) (2011) 7856–7862.

[13] E. Tarasova, V. Farafonov, M. Taiji, D. Nerukh, Details of charge distribution in stable viral capsid, J. Mol. Liq. 265 (2018) 585–591, https://doi.org/10.1016/j.molliq.2018.06.019.

[14] E. Tarasova, V. Farafonov, R. Khayat, N. Okimoto, T.S. Komatsu, M. Taiji, D. Nerukh, All-atom molecular dynamics simulations of entire virus capsid reveal the role of ion distribution in capsid's stability, J. Phys. Chem. Lett. 8 (2017) 779–784, https://doi.org/10.1021/acs.jpclett.6b02759.

[15] S.E. Mylon, C.I. Rinciog, N. Schmidt, L. Gutierrez, G.C.L. Wong, T.H. Nguyen, Influence of salts and natural organic matter on the s tability of bacteriophage MS2, Langmuir. 26 (2010) 1035–1042, https://doi.org/10.1021/la902290t.

[16] S. Watts, T.R. Julian, K. Maniura-Weber, T. Graule, S. Salentinig, Colloidal transformations in MS2 virus particles: driven by pH, influenced by natural organic matter, ACS Nano. 14 (2020) 1879–1887, https://doi.org/10.1021/acsnano.9b08112.

[17] C.P. Gerba, W.Q. Betancourt, Viral aggregation: impact on virus behavior in the environment, Environ. Sci. Technol. 51 (2017) 7318–7325, https://doi.org/10.1021/acs.est.6b05835.

[18] K. Lin, C.R. Schulte, L.C. Marr. Survival of MS2 and Φ6 viruses in droplets as a function of relative humidity, pH, and salt, protein, and surfactant concentrations. PLoS ONE 15(12) (2020) e0243505. Doi:10.1371/journal.pone.0243505.

[19] N.O. Mchedlov-Petrossyan, N.A. Vodolazkaya, Y.A. Gurina, W.-C. Sun, K.R. Gee, Medium effects on the prototropic equilibria of fluorescein fluoroderivatives in true and organized solution, J. Phys. Chem. 114 (2010) 4551–4564, https://doi.org/10.1021/jp909854s.

[20] N.O. Mchedlov-Petrossyan, N.A. Vodolazkaya, N.N. Kamneva. Acid-base equilibrium in aqueous micellar solutions of surfactants. In: Micelles: Structural Biochemistry, Formation and Functions and Usage. N. Y.: Nova Publishers, 2013. p. 321 (Chapter 1. – P. 1–71.).

[21] K. Vus, U. Tarabara, Z. Balklava, D. Nerukh, M. Stich, A. Laguta, N. Vodolazkaya, N. Mchedlov-Petrossyan, V. Farafonov, N. Kriklya, G. Gorbenko, V. Trusova, O. Zhytniakivska, A. Kurutos, N. Gadjev, T. Deligeorgiev, Association of novel monomethine cyanine dyes with bacteriophage MS2: a fluorescence study, J. Mol. Liq. 302 (2020), 112569, https://doi.org/10.1016/j.molliq.2020.112569.

[22] S.C. Gill, P.H. von Hippel, Calculation of protein extinction coefficients from amino acid sequence data, Analytical Biochemistry 182 (2) (1989) 319–326.

[23] S. Dhindwal, B. Avila, S. Feng, R. Khayat, Porcine Circovirus 2 uses a multitude of weak binding sites to interact with heparan sulfate, and the interactions do not follow the symmetry of the capsid, J Virol. 93 (6) (2019), https://doi.org/10.1128/JVI.02222-18 e02222-18.

[24] J.H. Waterborg, H.R. Matthews, The Lowry method for protein quantitation, Methods Mol. Biol. 1 (1984) 1–3, https://doi.org/10.1007/978-1-59745-198-7_2.

[25] D.A. Kuzmanovic, I. Elashvili, C.h. Wick, C. O'Connell, S. Krueger, Bacteriophage MS2: molecular weight and spatial distribution of the protein and RNA components by small-angle neutron scattering and virus counting, Structure. 11 (2003) 1339–1348, https://doi.org/10.1016/j.str.2003.09.021.

[26] C. Dika, C. Gantzer, A. Perrin, J.F.L. Duval, Impact of the virus purification protocol on aggregation and electrokinetics of MS2 phages and corresponding virus-like particles, Phys. Chem. Chem. Phys. 15 (2013) 5691–5700, https://doi.org/10.1039/c3cp44128h.

[27] M.H. Ly-Chatain, S. Moussaoui, A. Vera, V. Rigobello, Y. Demarigny, Antiviral effect of cationic compounds on bacteriophages, Frontiers in Microbiology. 4 (2013) 46, https://doi.org/10.3389/fmicb.2013.00046.

[28] G. Sautrey, A. Brie, C.h. Gantzer, A. Walcarius, MS2 and Qβ bacteriophages reveal the contribution of surface hydrophobicity on the mobility of non-enveloped icosahedral viruses in SDS-based capillary zone electrophoresis, Electrophoresis. 39 (2018) 377–385, https://doi.org/10.1002/elps.201700352.

[29] E.Y. Bryleva, N.A. Vodolazkaya, N.O. Mchedlov-Petrossyan, L.V. Samokhina, N. A. Matveevskaya, A.V. Tolmachev, Interfacial properties of cetyltrimethylammonium-coated SiO_2 nanoparticles in aqueous media as studied by using different indicator dyes, J. Coll. Interf. Sci. 316 (2007) 712–722, https://doi.org/10.1016/j.jcis.2007.07.036.

[30] B.S. Mertens, O.D. Velev, Characterization and control of surfactant-mediated Norovirus interactions, Soft Matter. 11 (2015) 8621–8631, https://doi.org/10.1039/c5sm01778e.

[31] D. Otzen, Protein–surfactant interactions: a tale of many states protein–surfactant interactions: a tale of many states, Biochimica et Biophysica Acta 2011 (1814) 562–591, https://doi.org/10.1016/j.bbapap.2011.03.003.

[32] E.V. Karamov, V.F. Larichev, G.V. Kornilaeva, I.T. Fedyakina, A.S. Turgiev, A. V. Shibaev, V.S. Molchanov, O.E. Philippova, A.R. Khokhlov, Cationic surfactants as disinfectants against SARS-CoV-2, Int. J. Mol. Sci. 23 (2022) 6645–6656, https://doi.org/10.3390/ijms23126645.

[33] V.S. Farafonov, M. Stich, D. Nerukh, Reconstruction and validation of entire virus model with complete genome from mixed resolution cryo-EM density, Faraday Discuss. 240 (2022) 152–167, https://doi.org/10.1039/D2FD00053A.